

## Origin of the unusually large band-gap bowing and the breakdown of the band-edge distribution rule in the $\text{Sn}_x\text{Ge}_{1-x}$ alloys

Wan-Jian Yin and Xin-Gao Gong

*Department of Physics and Surface Science Laboratory, Fudan University, Shanghai 200433, China*

Su-Huai Wei

*National Renewable Energy Laboratory, Golden, Colorado 80401, USA*

(Received 26 September 2008; published 24 October 2008)

The unusual nonlinear behaviors of the band gaps in  $\text{Sn}_x\text{Ge}_{1-x}$  alloys are investigated using first-principles calculations. We show that the large bowing of the direct band gap is induced by the disordering effect. Moreover, we calculated individual contribution of the band-edge states and found that the bowing of the conduction band edge is much larger than the bowing of the valence band edge, although the natural valence-band offset between Ge and Sn is larger than the natural conduction-band offset. The breakdown of the band-edge distribution rule is explained by the large lattice mismatch between Ge and Sn and the large deformation potential of the band-edge states.

DOI: 10.1103/PhysRevB.78.161203

PACS number(s): 71.22.+i, 71.20.Mq, 71.23.An

As the only direct band-gap material which is composed entirely of group IV elements, the  $\text{Sn}_x\text{Ge}_{1-x}$  alloy has attracted much attention in recent years.<sup>1-6</sup> It has been shown that the addition of Sn in Ge can enhance both the electron and hole mobilities,<sup>7</sup> thus, making the  $\text{Sn}_x\text{Ge}_{1-x}$  alloy a promising material for infrared optical detectors and high-speed integrated circuits. However, the electronic and optical properties of  $\text{Sn}_x\text{Ge}_{1-x}$  alloy exhibit several unusual behaviors that are not well understood. For example, most semiconductor alloys  $A_xB_{1-x}$  have a nonlinear dependence of its band gap  $E_g(x)$  as a function of the alloy composition  $x$ , and the variation is usually described by a parabolic function

$$E_g^{\text{alloy}}(x) = xE_g^A + (1-x)E_g^B - b_g x(1-x), \quad (1)$$

where  $E_g(A)$  and  $E_g(B)$  are the band gaps of  $A$  and  $B$  at their respective equilibrium lattice constants and  $b_g$  is the so-called bowing parameter. For  $\text{Sn}_x\text{Ge}_{1-x}$  alloy, several experimental studies<sup>1-3</sup> have confirmed that it has an unusually large band-gap bowing parameter ( $b_g \sim 2.6$  eV at low temperature)<sup>2</sup> for the direct band gap, i.e., much larger than the direct band gap of Ge ( $E_g^\Gamma = 0.9$  eV) or Sn ( $E_g^\Gamma = -0.4$  eV). On the other hand, all previous theoretical calculations<sup>8-10</sup> found that the band-gap bowing of  $\text{Sn}_x\text{Ge}_{1-x}$  alloys is small. For example, the virtual-crystal approximation (VCA) tight-binding calculation<sup>8</sup> gave  $b_g = 0.30$  eV, whereas the VCA pseudopotential calculation<sup>9</sup> found  $b_g = -0.40$  eV. First-principles calculation, using the zincblende (ZB)  $\text{Sn}_{0.5}\text{Ge}_{0.5}$  structure and modified potential, also predicted much smaller band-gap bowing ( $b_g = 0.58$  eV).<sup>10</sup> So far, the reason for the discrepancy between the experimental measurements and theoretical calculations is unknown.

Recently, Alberi *et al.*<sup>4</sup> proposed that the large bowing observed in the  $\text{Sn}_x\text{Ge}_{1-x}$  alloy could be described by a valence-band anticrossing model, which was originally proposed to explain the unusual variation of the conduction-band states in highly mismatched semiconductor alloys such as  $\text{GaAs}_{1-x}\text{N}_x$ .<sup>11</sup> In this model, they assumed that the ex-

tended Ge valence-band maximum (VBM) state coupled strongly to the localized Sn  $p$  orbital at 1.6 eV below the VBM, leading to a large upward bowing of  $b_{\text{VBM}} = -1.24$  eV for the VBM states and an approximately  $b_{\text{CBM}} = 0.7$  eV for the conduction-band minimum (CBM) state. Combining this result with their observation that the VBM shifts upward by  $dE_{\text{VBM}}/dx = 2.2$  eV, one would expect that the VBM offset between Ge and  $\alpha$ -Sn is about 1 eV. But in their analysis, they assumed the natural VBM offset is only 0.2 eV.<sup>4,12</sup>

From a theoretical point of view, the individual contribution of the VBM or CBM states to the band-gap bowing of an alloy has never been accurately determined. This is because such a determination requires accurate determination of the natural band offsets between the constituents and between the alloys. However, most previous calculations assumed that certain reference energy levels (e.g., average local pseudopotential or core-level energy) are independent of the lattice deformation, but the validity of these assumptions has not been proven.<sup>13</sup> Because of this, people often use the band-edge distribution rule to separate the contribution of VBM and CBM to the band-gap bowing. For the type-I system, this is given by<sup>4</sup>

$$b_{\text{VBM(CBM)}} = \frac{\Delta E_{\text{VBM(CBM)}}}{\Delta E_g} b_g, \quad (2)$$

where  $\Delta E_{\text{VBM}}$  and  $\Delta E_{\text{CBM}}$  are VBM and CBM natural band offsets. In Ref. 4, Alberi *et al.* assumed that the CBM and VBM offsets between Sn and Ge were  $-1.0$  and  $0.2$  eV, respectively, and  $b_g = 1.94$  eV. Using Eq. (2), one would expect that the magnitude of  $b_{\text{CBM}} = 1.62$  eV is much larger than  $b_{\text{VBM}} = -0.32$  eV,<sup>4</sup> which does not match the values they obtained from their valence-band anticrossing model with  $b_{\text{CBM}} = 0.70$  eV and  $b_{\text{VBM}} = -1.24$  eV. It is not clear whether these discrepancies are caused by the uncertainty in the band offsets, the invalidity of the band-edge distribution rule, or the valence-band anticrossing model for this system.

TABLE I. The lattice constant  $a$  (in Å) and atomic valence orbital energies  $\varepsilon_s$  and  $\varepsilon_p$  (in eV) calculated with GGA. The experimental values of lattice constants  $a_{\text{exp}}$  and Phillip electronegativity  $\chi$  are also presented.

	$a$	$a_{\text{exp}}$	$\varepsilon_s$	$\varepsilon_p$	$\chi$
Ge	5.64	5.66	-11.9123	-4.0398	1.35
Sn	6.45	6.49	-10.7652	-3.8557	1.15

In this study, using first-principles fully relativistic band-structure method and a more accurate approach that takes into account the core-level volume deformation (VD) potential, we find that the natural VBM offset between Ge and Sn is 0.91 eV, whereas the CBM offset is -0.41 eV (at low temperature). Moreover, using the same approach, we have calculated the band offsets between the  $\text{Sn}_x\text{Ge}_{1-x}$  alloys. Thus, the bowing contribution from the VBM and CBM states is accurately determined. We find that despite the fact that the natural VBM band offset between Ge and Sn is larger than the CBM offset, the CBM bowing is much larger than the bowing of the VBM state, indicating the breakdown of the band-edge distribution rule. This is explained by using the deformation potential and large lattice mismatch between Ge and Sn. We also find that the large band-gap bowing in the  $\text{Sn}_x\text{Ge}_{1-x}$  alloy is caused by alloy disorder. Our calculated bowing parameters,  $b_g$ , of disordered  $\text{Sn}_x\text{Ge}_{1-x}$  alloys are about 2.8 eV, which is very close to recent experimental values.<sup>3</sup> Using our calculated value, we expect the indirect-to-direct band-gap transition to take place at  $x \sim 0.063$  for disordered alloys, which is much less than the VCA predicted value of  $x \sim 0.21$ . The calculated spin-orbit splittings,  $\Delta_0$ , show little negative bowing, which is consistent with recent experiment.<sup>4</sup>

Our first-principles calculation is based on density-functional theory as implemented in the VASP code.<sup>14</sup> For the exchange-correlation functional, the generalized gradient approximation (GGA) of Perdew *et al.*<sup>15</sup> is used. The interaction between the core levels and valence electrons is included by the standard frozen-core projector augmented-wave (PAW) potentials provided within the VASP package.<sup>16</sup> The cut-off energy for the basis functions is 220 eV and the  $k$ -point sampling is  $8 \times 8 \times 8$  for the zinc-blende cell and equivalent  $k$  points for the supercell. The calculated lattice constants and atomic-orbital energies are presented in Table I. Our calculated lattice constants are in good agreement with experimental data.<sup>13</sup>

The absolute deformation potential (ADP)  $a_v^i = dE^i/d \ln V$  for state  $i$  describes the shift of an individual energy level  $E^i$  with respect to an absolute energy reference under a volume deformation. Previous calculations of valence-band offset, following the same experimental measurement procedure, assumed that the core-level ADP is negligible.<sup>17</sup> However, recent investigation of ADP shows that the ADP of core levels are not negligible.<sup>13</sup> Therefore, accurate band offset calculation has to take into account correctly the absolute volume deformation effect of the valence state. Using the lattice harmonic expansion approach,<sup>13</sup> our calculated ADPs for VBM and CBM states of Ge and Sn are listed in Table II.

TABLE II. The band-gap volume deformation potential  $dE_g/d \ln V$  and the absolute volume deformation potentials for VBM and CBM states (in eV) of Ge and Sn.

	$dE_g/d \ln V$	$dE_{\text{VBM}}/d \ln V$	$dE_{\text{CBM}}/d \ln V$
Ge	-9.06	2.26	-6.80
Sn	-6.88	1.55	-5.33

To calculate the *natural* valence-band offsets  $\Delta E_{\text{VBM}}$  between Ge and Sn, we first calculate the offsets at the average lattice constants between unrelaxed cubic Ge and Sn using the standard approach.<sup>17</sup> Afterward, we add to it the shift of the VBMs from the averaged lattice constants to the respective equilibrium lattice constants using the calculated ADPs given in Table II to obtain the natural valence-band offsets between Ge and Sn when they are both at their equilibrium lattice constants. The conduction-band offsets  $\Delta E_{\text{CBM}}$  are obtained using the relationship  $\Delta E_{\text{CBM}} = \Delta E_g + \Delta E_{\text{VBM}}$ , where  $\Delta E_g$  is the experimental band-gap difference between Ge and Sn. Our calculated band offsets are shown in Fig. 1. The calculated natural valence-band offset between Ge and Sn is 0.91 eV, which leads to a natural conduction-band offset of -0.41 eV at low temperature. Previous calculations following the same procedure as in the core-level photoemission measurement, i.e., assuming zero core-level ADP, find the valence-band offset to be 0.2 (Ref. 12) or 0.33 eV.<sup>18</sup> The difference indicates that for this system, the core-level ADP is significant. Figure 1 also shows that at the average lattice constants (or the lattice constant of the  $x=0.5$  alloy), the VBM offset is much smaller, whereas the CBM offset has an opposite sign and is much larger.

To calculate the electronic properties of random  $\text{Sn}_x\text{Ge}_{1-x}$  alloys, we use the special quasirandom structure (SQS) approach<sup>19</sup> and construct SQSs on a 64 atom  $2a \times 2a \times 2a$  cubic cell. In the SQS approach, the lattice sites are occupied

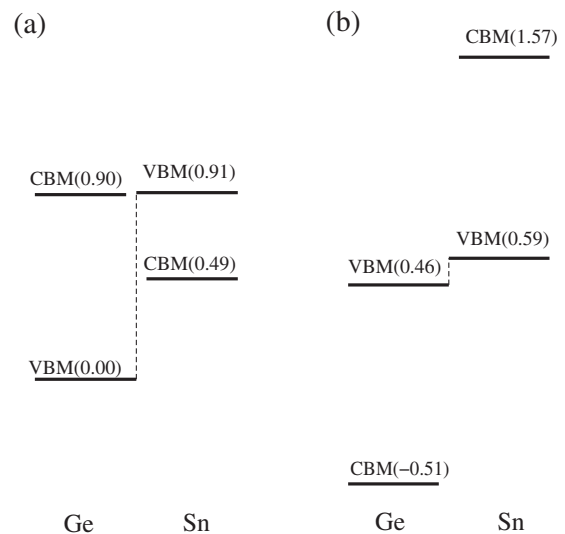


FIG. 1. Band lineups (in eV) of Ge and  $\alpha$ -Sn at (a) their respective equilibrium lattice constants and (b) alloy ( $x=0.5$ ) lattice constants. All energies refer to the VBM of Ge at equilibrium lattice constant.

TABLE III. Decomposed VD, CE, and SR bowing parameters (in eV) of  $\text{Sn}_x\text{Ge}_{1-x}$  alloy at  $x=0.25, 0.5$ , and  $0.75$ .

	$b_{\text{VD}}$	$b_{\text{CE}}$	$b_{\text{SR}}$	$b_{\text{total}}$
$x=0.25$				
Band gap	1.08	0.95	0.84	2.87
VBM	-0.40	-0.07	0.01	-0.46
CBM	0.68	0.88	0.85	2.41
$x=0.50$				
Band gap	0.93	0.72	0.85	2.50
VBM	-0.32	-0.01	0.02	-0.31
CBM	0.61	0.71	0.87	2.19
$x=0.75$				
Band gap	0.89	0.60	0.76	2.25
VBM	-0.28	-0.04	-0.03	-0.35
CBM	0.61	0.56	0.73	1.90

by Ge or Sn so that the structural correlation functions of the SQS mimic that of an infinite random alloy so the disorder effect is included. The SQS method was shown to be an efficient method to calculate physical properties of a random alloy.

In our calculations, we construct four  $\text{Sn}_x\text{Ge}_{1-x}$  SQS with  $x=0.125, 0.25, 0.50$ , and  $0.75$ . For each  $x$ , the lattice constants are obtained by total-energy minimization. To better understand the physical origin of  $\text{Sn}_x\text{Ge}_{1-x}$  direct band-gap bowing, we decompose the formation of  $\text{Sn}_x\text{Ge}_{1-x}$  alloys from pure Ge and Sn using a three-step process.<sup>20</sup> (i) Using the VD process, we compress Sn and dilate Ge from their equilibrium lattice constants to the alloy lattice constant. (ii) Using the chemical exchange (CE) process, we mix Ge and Sn atoms on perfect diamond lattice sites at the alloy lattice constant. (iii) With the structural relaxation (SR) process, we relax all the atomic positions inside the cell using quantum-mechanical forces. The VBM offsets between the alloys at different steps and the end-point constituents can be calculated using the same procedure described above. From that, the bowing parameters can be calculated. Table III gives the calculated bowing parameters for  $x=0.25, 0.5$ , and  $0.75$ , together with the contribution of the VBM and CBM, at the three steps. We observe the following results.

(i) The calculated band-gap bowings,  $b_g(x=0.125)=2.75$  eV,  $b_g(x=0.25)=2.87$  eV,  $b_g(x=0.50)=2.50$  eV, and  $b_g(x=0.75)=2.25$  eV, show only small composition dependence and, the results are in good agreement with experimental values of  $b_g \sim 2.84$  eV at low composition.<sup>3</sup> For comparison, the calculated bowing parameters for the low-energy ordered ZB or rhombohedra (RH) structures<sup>21</sup> ( $x=0.5$ ) are 1.22 and 0.92 eV, respectively. These results indicate that the failure of previous calculations to describe the bowing of  $\text{Sn}_x\text{Ge}_{1-x}$  alloys originates from the neglect of structural disorder. This is because in a semiconductor alloy, the band-gap bowing is caused by the coupling of states through non-diamond-like potential. For systems such as  $\text{Sn}_x\text{Ge}_{1-x}$  with large lattice mismatch between the constitu-

ents, it cannot be described properly by potential-averaged VCA or ZB/RH alloys that have high symmetry.

(ii) The bowing parameter of CBM is much larger than VBM, even though the natural VBM band offset of Ge and Sn is larger than CBM (Fig. 1). This is because although Ge and Sn have large natural VBM band offset and small natural CBM band offset, after the VD process, the situation is reversed—with small VBM band offset and large CBM band offset. The VD contribution of band-gap bowing is positive, indicating that the band-gap deformation potential of Ge is larger than Sn, which can also be seen in Table II. Obviously, Eq. (2) is inapplicable here if the natural band offsets are used as input because after the large volume deformation, the band alignment is very different from the natural band offsets. However, if we consider the band offsets after the VD process [Fig. 1(b)], then the results are qualitatively consistent with Eq. (2). This indicates that the breakdown of the band-edge distribution rule [Eq. (2)] is caused by the large lattice mismatch between Ge and Sn and by the large volume deformation potentials for the VBM and CBM states. It is also interesting to notice that the VBM has atomic  $p$ -orbital characters and the CBM has atomic  $s$ -orbital characters. Therefore, it is not surprising that the CBM makes a large contribution to the band-gap bowing because the atomic-orbital energy difference between the valence  $p$  orbitals is only 0.18 eV but it is 1.15 eV for the valence  $s$  orbitals (Table I).

(iii) The amounts of  $b_{\text{VD}}$ ,  $b_{\text{CE}}$ , and  $b_{\text{SR}}$  are comparable, which indicates that the large bowing of Ge and Sn is the joint effect of large lattice mismatch and electronegativity differences. This is different from the giant bowing mechanism of  $\text{GaAs}_{1-x}\text{N}_x$ , where the bowing is strongly composition dependent and  $b_{\text{CE}}$  and  $b_{\text{SR}}$  are dominant.<sup>22</sup>

(iv) The large direct band-gap bowing of  $\text{Sn}_x\text{Ge}_{1-x}$  alloys reduces the Sn concentration at which the indirect-to-direct band-gap transition happens. Using our calculated  $L$ - $\Gamma$  band-gap bowing,  $b_{L-\Gamma}=0.89$  eV, this transition will take place at  $x \sim 6.3\%$ . This is consistent with recent experimental indication that this transition occurs at  $0.06 < x < 0.10$ .<sup>3</sup> Previous experiments suggest that this transition may occur at a high value near 11%.<sup>1,2</sup> This may be due to the fact that the experimental samples used in these experiments have the tendency of being partially ordered because the ordered ZB or RH structures are strain free. This partial ordering can lead to a smaller bowing parameter and a larger direct-indirect transition composition. Figure 2 plots the band-gap variation as a function of Sn composition. We also find that for disordered  $\text{Sn}_x\text{Ge}_{1-x}$  alloys, the band gap disappears near  $x=0.29$ .

(v) We have also calculated the spin-orbit splitting  $\Delta_0$  of Ge, Sn, and the alloys. The results are shown in Table IV. We find a small negative bowing for  $\Delta_0$  because the VBM wave function is more localized on the Sn side with higher  $p$ -orbital energy (Table I).<sup>23</sup> Experimentally, the observed bowing for  $\Delta_0$  ranges from 0.32 eV in Ref. 2 to  $-0.1$  eV in Ref. 4.

In summary, our first-principles band-structure calculation revealed the mystery of the large band-gap bowing parameters of the  $\text{Sn}_x\text{Ge}_{1-x}$  alloy, showing that it is induced by the disordering effect. Moreover, using a more accurate approach that avoids unphysical assumptions in previous band

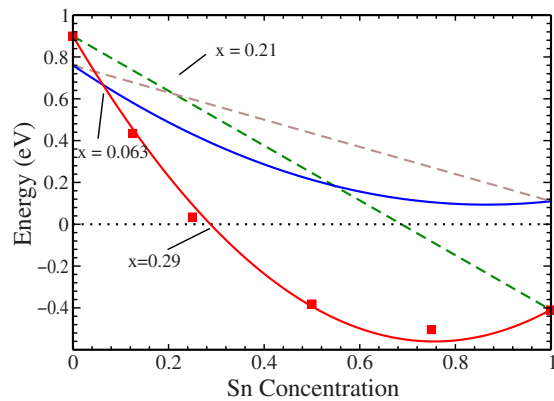


FIG. 2. (Color online) Direct  $\Gamma$ - $\Gamma$  band gap (red/gray line) and the indirect  $\Gamma$ - $L$  band gap (blue/dark gray line) of the disordered alloy as a function of Sn concentration. Green/light gray and brown/gray dashed lines are linear connections of  $\Gamma$ - $\Gamma$  and  $\Gamma$ - $L$  band gaps of Ge and  $\alpha$ -Sn at 0 K. The fitted bowing parameters for the  $\Gamma$ - $\Gamma$  and  $\Gamma$ - $L$  band gaps are 2.55 and 0.89 eV, respectively. The direct calculated results (solid squares) are also indicated.

offset calculations, we have accurately determined the band offsets between Sn and Ge, and between the  $\text{Sn}_x\text{Ge}_{1-x}$  alloys. This allows us to determine the individual contribution of VBM and CBM states to the band-gap bowing. We find that the natural valence-band offset between Ge and Sn is larger

TABLE IV. Calculated spin-orbital coupling  $\Delta_0$  and its bowing. All values are in eV.

Sn concentration	$\Delta_0$	$b_{\Delta_0}$
0 (Ge)	0.3026	
1/4	0.4242	-0.1253
1/2	0.5224	-0.0944
3/4	0.6029	-0.0320
1 ( $\alpha$ -Sn)	0.6950	

than the natural conduction-band offset, but the bowing of the CBM is much larger than the bowing of the VBM state. The breakdown of the band-edge distribution rule is explained by the large lattice mismatch between Ge and Sn and by the large deformation potential of the band-edge states. Our analysis and calculation approaches are general and applicable to other semiconductor alloys.

The work in Fudan University was partially supported by the Special Funds for Major State Basic Research, National Science Foundation of China. The computation was performed in the Supercomputer Center of Shanghai, the Supercomputer Center of Fudan University, and CCS. The work at NREL was funded by the U.S. Department of Energy under Contract No. DE-AC36-99GO10337.

<sup>1</sup>G. He and H. A. Atwater, Phys. Rev. Lett. **79**, 1937 (1997).

<sup>2</sup>V. R. D'Costa, C. S. Cook, A. G. Birdwell, C. L. Littler, M. Canonico, S. Zollner, J. Kouvetakis, and J. Menendez, Phys. Rev. B **73**, 125207 (2006).

<sup>3</sup>H. Perez Ladron de Guevara, A. G. Rodriguez, H. Navarro-Contreras, and M. A. Vidal, Appl. Phys. Lett. **91**, 161909 (2007).

<sup>4</sup>K. Alberi, J. Blacksberg, L. D. Bell, S. Nikzad, K. M. Yu, O. D. Dubon, and W. Walukiewicz, Phys. Rev. B **77**, 073202 (2008).

<sup>5</sup>J. Olajos, P. Vogl, W. Wegscheider, and G. Abstreiter, Phys. Rev. Lett. **67**, 3164 (1991).

<sup>6</sup>P. Zhang, V. H. Crespi, E. Chang, S. Louie, and M. Cohen, Nature (London) **409**, 69 (2001).

<sup>7</sup>J. D. Sau and M. L. Cohen, Phys. Rev. B **75**, 045208 (2007).

<sup>8</sup>D. W. Jenkins and J. D. Dow, Phys. Rev. B **36**, 7994 (1987).

<sup>9</sup>K. A. Mäder, A. Baldereschi, and H. von Kanel, Solid State Commun. **69**, 1123 (1989).

<sup>10</sup>T. Brudevoll, D. S. Citrin, N. E. Christensen, and M. Cardona, Phys. Rev. B **48**, 17128 (1993).

<sup>11</sup>W. Shan, W. Walukiewicz, J. W. Ager, E. E. Haller, J. F. Geisz, D. J. Friedman, J. M. Olson, and S. R. Kurtz, Phys. Rev. Lett.

**82**, 1221 (1999); K. M. Yu, W. Walukiewicz, J. Wu, W. Shan, J. W. Beeman, M. A. Scarpulla, O. D. Dubon, and P. Becla, *ibid.* **91**, 246403 (2003).

<sup>12</sup>R. S. Bauer and G. Margaritondo, Phys. Today **40**(1), 26 (1987).

<sup>13</sup>Y. H. Li, X. G. Gong, and S.-H. Wei, Appl. Phys. Lett. **88**, 042104 (2006); Phys. Rev. B **73**, 245206 (2006).

<sup>14</sup>G. Kresse and J. Furthmuller, Phys. Rev. B **54**, 11169 (1996).

<sup>15</sup>J. P. Perdew, J. A. Chevary, S. H. Vosko, K. A. Jackson, M. R. Pederson, D. J. Singh, and C. Fiolhais, Phys. Rev. B **46**, 6671 (1992).

<sup>16</sup>P. E. Blochl, Phys. Rev. B **50**, 17953 (1994); G. Kresse and D. Joubert, *ibid.* **59**, 1758 (1999).

<sup>17</sup>S.-H. Wei and A. Zunger, Phys. Rev. B **60**, 5404 (1999).

<sup>18</sup>S.-H. Wei, Comput. Mater. Sci. **30**, 337 (2004).

<sup>19</sup>S.-H. Wei, L. G. Ferreira, J. E. Bernard, and A. Zunger, Phys. Rev. B **42**, 9622 (1990).

<sup>20</sup>J. E. Bernard and A. Zunger, Phys. Rev. B **34**, 5992 (1986).

<sup>21</sup>J. L. Martins and A. Zunger, Phys. Rev. Lett. **56**, 1400 (1986).

<sup>22</sup>S.-H. Wei and A. Zunger, Phys. Rev. Lett. **76**, 664 (1996).

<sup>23</sup>S.-H. Wei and A. Zunger, Phys. Rev. B **39**, 6279 (1989).